

Measurement of the Top Quark Mass and $t\bar{t}$ Production Cross Section from Dilepton Events at the Collider Detector at Fermilab

- F. Abe,¹⁷ H. Akimoto,³⁹ A. Akopian,³¹ M. G. Albrow,⁷ A. Amadon,⁵ S. R. Amendolia,²⁷ D. Amidei,²⁰ J. Antos,³³ S. Aota,³⁷ G. Apollinari,³¹ T. Arisawa,³⁹ T. Asakawa,³⁷ W. Ashmanskas,¹⁸ M. Atac,⁷ P. Azzi-Bacchetta,²⁵ N. Bacchetta,²⁵ S. Bagdasarov,³¹ M. W. Bailey,²² P. de Barbaro,³⁰ A. Barbaro-Galtieri,¹⁸ V. E. Barnes,²⁹ B. A. Barnett,¹⁵ M. Barone,⁹ G. Bauer,¹⁹ T. Baumann,¹¹ F. Bedeschi,²⁷ S. Behrends,³ S. Belforte,²⁷ G. Bellettini,²⁷ J. Bellinger,⁴⁰ D. Benjamin,³⁵ J. Bensinger,³ A. Beretvas,⁷ J. P. Berge,⁷ J. Berryhill,⁵ S. Bertolucci,⁹ S. Bettelli,²⁷ B. Bevensee,²⁶ A. Bhatti,³¹ K. Biery,⁷ C. Bigongiari,²⁷ M. Binkley,⁷ D. Bisello,²⁵ R. E. Blair,¹ C. Blocker,³ S. Blusk,³⁰ A. Bodek,³⁰ W. Bokhari,²⁶ G. Bolla,²⁹ Y. Bonushkin,⁴ D. Bortoletto,²⁹ J. Boudreau,²⁸ L. Breccia,² C. Bromberg,²¹ N. Bruner,²² R. Brunetti,² E. Buckley-Geer,⁷ H. S. Budd,³⁰ K. Burkett,²⁰ G. Busetto,²⁵ A. Byon-Wagner,⁷ K. L. Byrum,¹ M. Campbell,²⁰ A. Caner,²⁷ W. Carithers,¹⁸ D. Carlsmith,⁴⁰ J. Cassada,³⁰ A. Castro,²⁵ D. Cauz,³⁶ A. Cerri,²⁷ P. S. Chang,³³ P. T. Chang,³³ H. Y. Chao,³³ J. Chapman,²⁰ M.-T. Cheng,³³ M. Chertok,³⁴ G. Chiarelli,²⁷ C. N. Chiou,³³ F. Chlebana,⁷ L. Christofek,¹³ M. L. Chu,³³ S. Chigangir,⁷ A. G. Clark,¹⁰ M. Cobal,²⁷ E. Cocco,²⁷ M. Contreras,⁵ J. Conway,³² J. Cooper,⁷ M. Cordelli,⁹ D. Costanzo,²⁷ C. Couyoumtzelis,¹⁰ D. Cronin-Hennessy,⁶ R. Culbertson,⁵ D. Dagenhart,³⁸ T. Daniels,¹⁹ F. DeJongh,⁷ S. Dell'Agnello,⁹ M. Dell'Orso,²⁷ R. Demina,⁷ L. Demortier,³¹ M. Deninno,² P. F. Derwent,⁷ T. Devlin,³² J. R. Dittmann,⁶ S. Donati,²⁷ J. Done,³⁴ T. Dorigo,²⁵ N. Eddy,²⁰ K. Einsweiler,¹⁸ J. E. Elias,⁷ R. Ely,¹⁸ E. Engels, Jr.,²⁸ W. Erdmann,⁷ D. Errede,¹³ S. Errede,¹³ Q. Fan,³⁰ R. G. Feild,⁴¹ Z. Feng,¹⁵ C. Ferretti,²⁷ I. Fiori,² B. Flaugh,⁷ G. W. Foster,⁷ M. Franklin,¹¹ J. Freeman,⁷ J. Friedman,¹⁹ H. Frisch,⁵ Y. Fukui,¹⁷ S. Gadomski,¹⁴ S. Galeotti,²⁷ M. Gallinaro,²⁶ O. Ganel,³⁵ M. Garcia-Sciveres,¹⁸ A. F. Garfinkel,²⁹ C. Gay,⁴¹ S. Geer,⁷ D. W. Gerdes,¹⁵ P. Giannetti,²⁷ N. Giokaris,³¹ P. Giromini,⁹ G. Giusti,²⁷ M. Gold,²² A. Gordon,¹¹ A. T. Goshaw,⁶ Y. Gotra,²⁵ K. Goulianios,³¹ H. Grassmann,³⁶ L. Groer,³² C. Grossi-Pilcher,⁵ G. Guilliam,²⁰ J. Guimaraes da Costa,¹⁵ R. S. Guo,³³ C. Haber,¹⁸ E. Hafner,¹⁹ S. R. Hahn,⁷ R. Hamilton,¹¹ T. Handa,¹² R. Handler,⁴⁰ F. Happacher,⁹ K. Hara,³⁷ A. D. Hardman,²⁹ R. M. Harris,⁷ F. Hartmann,¹⁶ J. Hauser,⁴ E. Hayashi,³⁷ J. Heinrich,²⁶ W. Hao,³⁵ B. Hinrichsen,¹⁴ K. D. Hoffman,²⁹ M. Hohlmann,⁵ C. Holck,²⁶ R. Hollebeek,²⁶ L. Holloway,¹³ Z. Huang,²⁰ B. T. Huffman,²⁸ R. Hughes,²³ J. Huston,²¹ J. Huth,¹¹ H. Ikeda,³⁷ M. Incagli,²⁷ J. Incandela,⁷ G. Introzzi,²⁷ J. Iwai,³⁹ Y. Iwata,¹² E. James,²⁰ H. Jensen,⁷ U. Joshi,⁷ E. Kajfasz,²⁵ H. Kambara,¹⁰ T. Kamon,³⁴ T. Kaneko,³⁷ K. Karr,³⁸ H. Kasha,⁴¹ Y. Kato,²⁴ T. A. Keaffaber,²⁹ K. Kelley,¹⁹ R. D. Kennedy,⁷ R. Kephart,⁷ D. Kestenbaum,¹¹ D. Khazins,⁶ T. Kikuchi,³⁷ B. J. Kim,²⁷ H. S. Kim,¹⁴ S. H. Kim,³⁷ Y. K. Kim,¹⁸ L. Kirsch,³ S. Klimentko,⁸ D. Knoblauch,¹⁶ P. Koehn,²³ A. Kongeter,¹⁶ K. Kondo,³⁷ J. Konigsberg,⁸ K. Kordas,¹⁴ A. Korytov,⁸ E. Kovacs,¹ W. Kowald,⁶ J. Kroll,²⁶ M. Kruse,³⁰ S. E. Kuhlmann,¹ E. Kuns,³² K. Kurino,¹² T. Kuwabara,³⁷ A. T. Laasanen,²⁹ S. Lami,²⁷ S. Lammel,⁷ J. I. Lamoureux,³ M. Lancaster,¹⁸ M. Lanzoni,²⁷ G. Latino,²⁷ T. LeCompte,¹ S. Leone,²⁷ J. D. Lewis,⁷ P. Limon,⁷ M. Lindgren,⁴ T. M. Liss,¹³ J. B. Liu,³⁰ Y. C. Liu,³³ N. Lockyer,²⁶ O. Long,²⁶ C. Loomis,³² M. Loreti,²⁵ D. Lucchesi,²⁷ P. Lukens,⁷ S. Lusin,⁴⁰ J. Lys,¹⁸ K. Maeshima,⁷ P. Maksimovic,¹⁹ M. Mangano,²⁷ M. Mariotti,²⁵ J. P. Marriner,⁷ A. Martin,⁴¹ J. A. J. Matthews,²² P. Mazzanti,² P. McIntyre,³⁴ P. Melese,³¹ M. Meguzzato,²⁵ A. Menzione,²⁷ E. Meschi,²⁷ S. Metzler,²⁶ C. Miao,²⁰ T. Miao,⁷ G. Michail,¹¹ R. Miller,²¹ H. Minato,³⁷ S. Miscetti,⁹ M. Mishina,¹⁷ S. Miyashita,³⁷ N. Moggi,²⁷ E. Moore,²² Y. Morita,¹⁷ A. Mukherjee,⁷ T. Muller,¹⁶ P. Murat,²⁷ S. Murgia,²¹ H. Nakada,³⁷ I. Nakano,¹² C. Nelson,⁷ D. Neuberger,¹⁶ C. Newman-Holmes,⁷ C.-Y. P. Ngan,¹⁹ L. Nodulman,¹ A. Nomerotski,⁸ S. H. Oh,⁶ T. Ohmoto,¹² T. Ohsugi,¹² R. Oishi,³⁷ M. Okabe,³⁷ T. Okusawa,²⁴ J. Olsen,⁴⁰ C. Pagliarone,²⁷ R. Paoletti,²⁷ V. Papadimitriou,³⁵ S. P. Pappas,⁴¹ N. Parashar,²⁷ A. Parri,⁹ J. Patrick,⁷ G. Paulette,³⁶ M. Paulini,¹⁸ A. Perazzo,²⁷ L. Pescara,²⁵ M. D. Peters,¹⁸ T. J. Phillips,⁶ G. Piacentino,²⁷ M. Pillai,³⁰ K. T. Pitts,⁷ R. Plunkett,⁷ L. Pondrom,⁴⁰ J. Proudfoot,¹ F. Ptchos,¹¹ G. Punzi,²⁷ K. Ragan,¹⁴ D. Reher,¹⁸ M. Reischl,¹⁶ A. Ribon,²⁵ F. Rimondi,² L. Ristori,²⁷ W. J. Robertson,⁶ T. Rodrigo,²⁷ S. Rolli,³⁸ L. Rosenson,¹⁹ R. Roser,¹³ T. Saab,¹⁴ W. K. Sakamoto,³⁰ D. Saltzberg,⁴ A. Sansoni,⁹ L. Santi,³⁶ H. Sato,³⁷ P. Schlabach,⁷ E. E. Schmidt,⁷ M. P. Schmidt,⁴¹ A. Scott,⁴ A. Scribano,²⁷ S. Segler,⁷ S. Seidel,²² Y. Seiya,³⁷ F. Semeria,² T. Shah,¹⁹ M. D. Shapiro,¹⁸ N. M. Shaw,²⁹ P. F. Shepard,²⁸ T. Shibayama,³⁷ M. Shimojima,³⁷ M. Shochet,⁵ J. Siegrist,¹⁸ A. Sill,³⁵ P. Sinervo,¹⁴ P. Singh,¹³ K. Sliwa,³⁸ C. Smith,¹⁵ F. D. Snider,¹⁵ J. Spalding,⁷ T. Speer,¹⁰ P. Sphicas,¹⁹ F. Spinella,²⁷ M. Spiropulu,¹¹ L. Spiegel,⁷ L. Stanco,²⁵ J. Steele,⁴⁰ A. Stefanini,²⁷ R. Ströhmer,^{7*} J. Strologas,¹⁰ F. Strumia,¹⁰ D. Stuart,⁷ K. Sumorok,¹⁹ J. Suzuki,³⁷ T. Suzuki,³⁷ T. Takahashi,²⁴ T. Takano,²⁴ R. Takashima,¹² K. Takikawa,³⁷ M. Tanaka,³⁷ B. Tannenbaum,²² F. Tartarelli,²⁷ W. Taylor,¹⁴ M. Tecchio,²⁰ P. K. Teng,³³ Y. Teramoto,²⁴ K. Terashi,³⁷ S. Tether,¹⁹ D. Theriot,⁷ T. L. Thomas,²² R. Thurman-Keup,¹

M. Timko,³⁸ P. Tipton,³⁰ A. Titov,³¹ S. Tkaczyk,⁷ D. Toback,⁵ K. Tollefson,¹⁹ A. Tollestrup,⁷ H. Toyoda,²⁴
 W. Trischuk,¹⁴ J. F. de Troconiz,¹¹ S. Truitt,²⁰ J. Tseng,¹⁹ N. Turini,²⁷ T. Uchida,³⁷ F. Ukegawa,²⁶ J. Valls,³²
 S. C. van den Brink,²⁸ S. Vejcik III,²⁰ G. Velev,²⁷ R. Vidal,⁷ R. Vilar,^{7,*} D. Vucinic,¹⁹ R. G. Wagner,¹ R. L. Wagner,⁷
 J. Wahl,⁵ N. B. Wallace,²⁷ A. M. Walsh,³² C. Wang,⁶ C. H. Wang,³³ M. J. Wang,³³ A. Warburton,¹⁴ T. Watanabe,³⁷
 T. Watts,³² R. Webb,³⁴ C. Wei,⁶ H. Wenzel,¹⁶ W. C. Wester III,⁷ A. B. Wicklund,¹ E. Wicklund,⁷ R. Wilkinson,²⁶
 H. H. Williams,²⁶ P. Wilson,⁵ B. L. Winer,²³ D. Winn,²⁰ D. Wolinski,²⁰ J. Wolinski,²¹ S. Worm,²² X. Wu,¹⁰ J. Wyss,²⁷
 A. Yagil,⁷ W. Yao,¹⁸ K. Yasuoka,³⁷ G. P. Yeh,⁷ P. Yeh,³³ J. Yoh,⁷ C. Yosef,²¹ T. Yoshida,²⁴ I. Yu,⁷ A. Zanetti,³⁶
 F. Zetti,²⁷ and S. Zucchelli²

(CDF Collaboration)

¹Argonne National Laboratory, Argonne, Illinois 60439

²Istituto Nazionale di Fisica Nucleare, University of Bologna, I-40127 Bologna, Italy

³Brandeis University, Waltham, Massachusetts 02254

⁴University of California at Los Angeles, Los Angeles, California 90024

⁵University of Chicago, Chicago, Illinois 60637

⁶Duke University, Durham, North Carolina 27708

⁷Fermi National Accelerator Laboratory, Batavia, Illinois 60510

⁸University of Florida, Gainesville, Florida 32611

⁹Laboratori Nazionali di Frascati, Istituto Nazionale di Fisica Nucleare, I-00044 Frascati, Italy

¹⁰University of Geneva, CH-1211 Geneva 4, Switzerland

¹¹Harvard University, Cambridge, Massachusetts 02138

¹²Hiroshima University, Higashi-Hiroshima 724, Japan

¹³University of Illinois, Urbana, Illinois 61801

¹⁴Institute of Particle Physics, McGill University, Montreal H3A 2T8

and University of Toronto, Toronto M5S 1A7, Canada

¹⁵The Johns Hopkins University, Baltimore, Maryland 21218

¹⁶Institut für Experimentelle Kernphysik, Universität Karlsruhe, 76128 Karlsruhe, Germany

¹⁷National Laboratory for High Energy Physics (KEK), Tsukuba, Ibaraki 305, Japan

¹⁸Ernest Orlando Lawrence Berkeley National Laboratory, Berkeley, California 94720

¹⁹Massachusetts Institute of Technology, Cambridge, Massachusetts 02139

²⁰University of Michigan, Ann Arbor, Michigan 48109

²¹Michigan State University, East Lansing, Michigan 48824

²²University of New Mexico, Albuquerque, New Mexico 87131

²³The Ohio State University, Columbus, Ohio 43210

²⁴Osaka City University, Osaka 588, Japan

²⁵Università di Padova, Istituto Nazionale di Fisica Nucleare, Sezione di Padova, I-35131 Padova, Italy

²⁶University of Pennsylvania, Philadelphia, Pennsylvania 19104

²⁷Istituto Nazionale di Fisica Nuclear, University and Scuola Normale Superiore di Pisa, I-56100 Pisa, Italy

²⁸University of Pittsburgh, Pittsburgh, Pennsylvania 15260

²⁹Purdue University, West Lafayette, Indiana 47907

³⁰University of Rochester, Rochester, New York 14627

³¹Rockefeller University, New York, New York 10021

³²Rutgers University, Piscataway, New Jersey 08855

³³Academia Sinica, Taipei, Taiwan 11530, Republic of China

³⁴Texas A&M University, College Station, Texas 77843

³⁵Texas Tech University, Lubbock, Texas 79409

³⁶Istituto Nazionale di Fisica Nucleare, University of Trieste/Udine, Italy

³⁷University of Tsukuba, Tsukuba, Ibaraki 315, Japan

³⁸Tufts University, Medford, Massachusetts 02155

³⁹Waseda University, Tokyo 169, Japan

⁴⁰University of Wisconsin, Madison, Wisconsin 53706

⁴¹Yale University, New Haven, Connecticut 06520

(Received 30 September 1997)

We present an analysis of dilepton events originating from $t\bar{t}$ production in $p\bar{p}$ collisions at $\sqrt{s} = 1.8$ TeV at the Fermilab Tevatron Collider. The sample corresponds to an integrated luminosity of $109 \pm 7 \text{ pb}^{-1}$. We observe nine candidate events, with an estimated background of 2.4 ± 0.5 events. We determine the mass of the top quark to be $M_{\text{top}} = 161 \pm 17(\text{stat}) \pm 10(\text{syst}) \text{ GeV}/c^2$. In addition, we measure a $t\bar{t}$ production cross section of $8.2^{+4.4}_{-3.4} \text{ pb}$ (where $M_{\text{top}} = 175 \text{ GeV}/c^2$ has been assumed for the acceptance estimate). [S0031-9007(98)05579-3]

PACS numbers: 14.65.Ha, 13.85.Ni, 13.85.Qk

We report here on a measurement of the $t\bar{t}$ production cross section and top quark mass in the dilepton channel with the Collider Detector at Fermilab (CDF). The data sample corresponds to a total integrated luminosity of $109 \pm 7 \text{ pb}^{-1}$. This analysis considers dilepton events originating predominantly from $t\bar{t} \rightarrow W^+ b W^- \bar{b} \rightarrow (\ell^+ \nu b) (\ell^- \bar{\nu} \bar{b})$, with $\ell = e$ or μ . A subset of these events corresponding to a data sample of 67 pb^{-1} supported the discovery of the top quark [1,2].

Recently both the CDF and D0 collaborations have updated their measurements of the $t\bar{t}$ production cross section [3,4] and top quark mass [5,6] using the “lepton plus jets” channel: $t\bar{t} \rightarrow W^+ b W^- \bar{b} \rightarrow (\ell^+ \nu b) (q\bar{q}'\bar{b})$, with $\ell = e$ or μ , which has larger statistics. The consistency of the measurements presented here with those in the lepton plus jets channel is an important confirmation that these two orthogonal sets of events originate from the same heavy top production process.

A description of the CDF detector can be found in Ref. [7]. The coordinate system and various quantities used throughout this paper are defined in [8]. The momenta of the charged leptons are measured with the central tracking chamber in a 1.4 T superconducting solenoidal magnet. Electromagnetic and hadronic calorimeters surrounding the tracking chambers are used to identify and measure the energies of electrons and jets. Muons are identified with drift chambers located outside the calorimeters. A three-level trigger selects high transverse momentum (P_T) electrons and muons.

The event selection is very similar to the previous analysis described in Refs. [1,9]. We require two high- P_T ($P_T > 20 \text{ GeV}/c$), oppositely charged leptons (e or μ) in the central pseudorapidity region ($|\eta| < 1.0$) with at least one of them well isolated from nearby tracks and calorimeter activity. We reject $Z \rightarrow \ell^+ \ell^- X$ events by requiring the dilepton invariant mass, M_{ee} or $M_{\mu\mu}$, to be outside the interval 75 – $105 \text{ GeV}/c^2$. If there is a high transverse energy ($E_T > 10 \text{ GeV}$) isolated photon present, the event is removed if consistent with a radiative Z decay. We also require that there be at least two jets with measured $E_T > 10 \text{ GeV}$ in the pseudorapidity range $|\eta| < 2.0$, as expected from the presence of two b quarks in a $t\bar{t}$ event. The signature of the two neutrinos in the decay is the missing energy transverse to the beam direction (\cancel{E}_T); we require $|\cancel{E}_T| > 25 \text{ GeV}$. The \cancel{E}_T is corrected for nonuniformities in calorimeter response and absolute energy scale, and for high- P_T muons. To ensure that the \cancel{E}_T is not due to mismeasurements of the energies of the leptons or jets, we require $|\cancel{E}_T| > 50 \text{ GeV}$ if the azimuthal angle between the direction of the \cancel{E}_T vector and the nearest lepton or jet (j), $\Delta\phi(\cancel{E}_T, \ell \text{ or } j)$, is less than 20° [9].

The distribution of $\Delta\phi(\cancel{E}_T, \ell \text{ or } j)$ versus $|\cancel{E}_T|$ is shown in Fig. 1 for dilepton events that pass the invariant mass and two-jet requirements. Superimposed is the expected distribution from the HERWIG [10] $t\bar{t}$ Monte Carlo program for $M_{\text{top}} = 175 \text{ GeV}/c^2$ followed by a

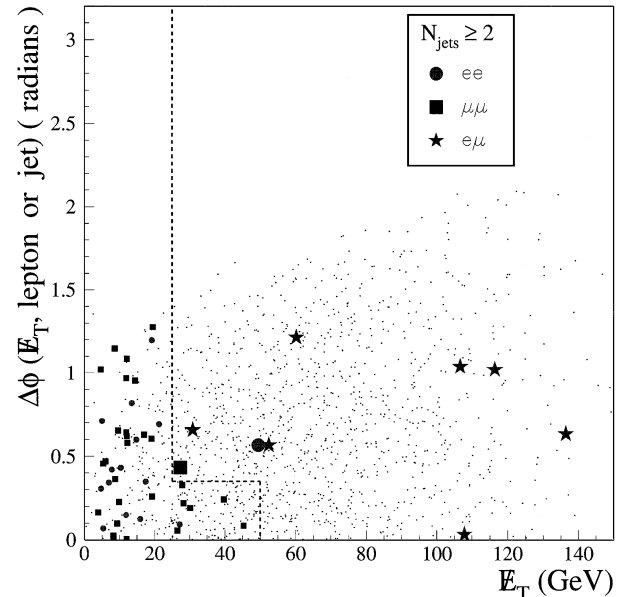


FIG. 1. Azimuthal angle between \cancel{E}_T and the nearest lepton or jet versus $|\cancel{E}_T|$ for events with two leptons and two jets. The dashed line represents the \cancel{E}_T cut. The small dots are for $t\bar{t}$ Monte Carlo for $M_{\text{top}} = 175 \text{ GeV}/c^2$ and corresponds to an integrated luminosity of about 24 fb^{-1} . The larger symbols represent the data.

detector simulation. (The top mass value of $175 \text{ GeV}/c^2$ is used to be consistent with CDF’s most precise mass measurements, that from the lepton plus jets channel [5].) We find nine candidate events in the signal region: seven $e\mu$, one $\mu\mu$, and one ee event.

The identification efficiencies for single leptons are measured from $Z \rightarrow \ell^+ \ell^-$ events in the data and are found to be 91% for muons and 83% for electrons [11]. The acceptance for $t\bar{t}$ decays to pass all of the selection criteria, including lepton identification, is the average of the results from the HERWIG and PYTHIA [12] Monte Carlo programs followed by a detector simulation. We find for $M_{\text{top}} = 175 \text{ GeV}/c^2$ that $(0.74 \pm 0.08)\%$ of all $t\bar{t}$ decays pass the above dilepton selection criteria. The uncertainty is dominated by the differences between the event generators and by the systematic uncertainties in the detector simulation. The acceptance increases by 35% as M_{top} increases from 150 to 200 GeV/c^2 . In $(86 \pm 2)\%$ of the dilepton events passing all selection criteria, both leptons come directly from the decays of the W bosons. The remainder consists mostly of events in which one of the W bosons decays to a τ lepton, which in turn decays to an electron or muon. Of the dilepton events, we expect $(58 \pm 2)\%$ to be $e\mu$, $(27 \pm 1)\%$ $\mu\mu$ and $(15 \pm 1)\%$ ee , where the uncertainty is statistical only. Using a $t\bar{t}$ production cross section value of 5.5 pb , consistent with recent theoretical calculations [13] that assume $M_{\text{top}} = 175 \text{ GeV}/c^2$, we expect to observe 4.4 signal events.

As backgrounds we consider standard model processes, other than $t\bar{t}$, which can result in dilepton final states. The main sources are Drell-Yan ($Z^*/\gamma \rightarrow ee, \mu\mu$), $Z \rightarrow \tau\tau$,

and WW production. If these events contain additional jets from QCD radiation plus \cancel{E}_T , either from real neutrinos or from energy mismeasurement, they may satisfy our selection criteria. Background contributions from radiative Z bosons and from $b\bar{b}$, WZ , ZZ , and $Wb\bar{b}$ production are estimated to be small. Additional sources are processes with a real lepton and a jet or a track faking a second lepton, and processes in which mismeasured muon tracks can result in an overestimate of the \cancel{E}_T in the event. This latter background is not relevant for electrons because the electron energy is measured in the calorimeters. We estimate the background from Drell-Yan production, fake leptons, and mismeasured tracks from the data; the other backgrounds are calculated using Monte Carlo simulations. The background contributions from the different sources are listed in Table I. The errors include both systematic and statistical uncertainties. Of the 2.4 ± 0.5 total background events estimated, 0.8 ± 0.2 are expected in the $e\mu$ channel, which does not have a contribution from Drell-Yan production, the dominant background source in the ee and $\mu\mu$ channels.

When relaxing the two-jet requirement in the data selection, we find eight dilepton events with zero jets and eleven with one jet, while we expect 8 ± 2 and 7 ± 2 events, respectively, from both background and $t\bar{t}$. The $t\bar{t}$ contribution is small; using the measured $t\bar{t}$ production cross section in this channel (see below), we expect 0.03 ± 0.02 dilepton events in the zero jet sample and 1.1 ± 0.5 events with one jet. Of the eleven events in the data with one jet, four are dimuons, three of which show the expected characteristics of the mismeasured muon track background. The expectation from this background is 1.4 ± 1.5 events. Five of the remaining seven events are $e\mu$. One of these five events has a jet tagged as a b quark (see below). The expected number of $t\bar{t}$ events in the one jet sample with the jet tagged as a b quark is about 0.2.

We find two events in the data that satisfy all selection criteria, except for the opposite sign requirement on the lepton charge. We expect 0.37 ± 0.23 same sign dilepton plus two-jet events from fake lepton background and 0.24 ± 0.11 from $t\bar{t}$. Without any jet requirements these estimates are 2.6 ± 1.9 and 0.29 ± 0.13 , respectively. There are no events in the data with two same sign leptons and zero or one jets that satisfy all of the other selection criteria.

TABLE I. Expected dilepton backgrounds in $109 \pm 7 \text{ pb}^{-1}$.

Background type	Expected No. of events
Drell-Yan	0.61 ± 0.30
$Z \rightarrow \tau\tau$	0.59 ± 0.14
Fake leptons	0.37 ± 0.23
WW	0.36 ± 0.11
Mismeasured muon tracks	0.3 ± 0.3
$b\bar{b}$	0.05 ± 0.03
Other (radiative Z , $Wb\bar{b}$, WZ , ZZ)	0.1 ± 0.1
Total	2.4 ± 0.5

Events originating from $t\bar{t}$ decays are characterized by the presence of jets originating from b quarks. Four of the nine candidate events have one jet tagged as a b quark, as evidenced by the presence of a secondary vertex in the silicon vertex detector (SVX tag) [9]. Two of these four jets are also tagged by a soft lepton from the semileptonic decay of the b quark (SLT tag) [9]. No jets are found to be tagged by the SLT method alone. In a sample of seven $t\bar{t}$ events, 4.3 ± 0.4 jets are expected to be tagged by at least one of the two tagging methods. If all nine candidates were from background processes, the number of expected b -tagged jets would be 0.7 ± 0.2 .

Using the nine observed dilepton events, 2.4 ± 0.5 of which are estimated to be background, an overall acceptance of $(0.74 \pm 0.08)\%$ (for $M_{\text{top}} = 175 \text{ GeV}/c^2$), and an integrated luminosity of $109 \pm 7 \text{ pb}^{-1}$, we calculate the $t\bar{t}$ production cross section to be $8.2^{+4.4}_{-3.4} \text{ pb}$.

With $t\bar{t}$ dilepton decays, reconstructing the top quark mass from the measured final state is a kinematically under-constrained problem due to the presence of two neutrinos.

To increase the purity of the sample for the mass analyses, we require $H_T > 170 \text{ GeV}$. H_T is defined as the sum of the P_T 's of the two leptons (E_T for electrons), the E_T 's of the two highest E_T jets and the $|\cancel{E}_T|$. For the nine candidate events the H_T distribution is shown in Fig. 2, together with the expectations from a Monte Carlo calculation for $M_{\text{top}} = 175 \text{ GeV}/c^2$ and background. The efficiency of the $H_T > 170 \text{ GeV}$ cut is about 95% for $M_{\text{top}} = 175 \text{ GeV}/c^2$. After this cut, eight of the nine dilepton candidate events survive and the background is reduced to 1.3 ± 0.3 events.

We present two methods to determine the top quark mass. The first method takes advantage of the correlation between the energy of the jets from b quarks in top quark decays and the top quark mass. From Monte Carlo simulation of $t\bar{t}$ decays we find that the mean energy of the two highest E_T jets increases linearly with M_{top} with a slope of 0.5. We obtain the most probable value of M_{top} for our set of events by comparing the observed distribution of jet energies with Monte Carlo distributions (templates) for different top quark masses.

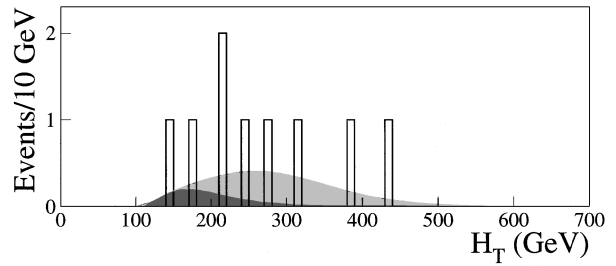


FIG. 2. Comparison of H_T for the candidate events (histogram) and the expectation from $t\bar{t}$ production ($M_{\text{top}} = 175 \text{ GeV}/c^2$) plus background (lighter shaded area). The background distribution alone is represented by the darker shaded area.

We use the two highest E_T jets in the event. The jet energies are corrected for nonuniformities in calorimeter response and absolute energy scale. The templates for $t\bar{t}$ decays are obtained from large samples of Monte Carlo events generated with HERWIG, and reconstructed with the same analysis programs as the data. Templates are also obtained for the background processes discussed above. The top quark mass is estimated by performing a maximum likelihood fit of the jet energy distribution from the data to a combination of $t\bar{t}$ and background templates. The amount of background is constrained to the expected value within its uncertainty. From the resulting likelihood values \mathcal{L}_m , for each assumed top quark mass m , the negative logarithms $-\ln(\mathcal{L}_m)$ are fit with a third order polynomial and the value of the mass corresponding to the minimum of the polynomial is obtained. The statistical uncertainties are determined by the values of the mass that give an increase of 0.5 in $-\ln(\mathcal{L}_m)$ from the minimum.

We have tested the fitting method with many Monte Carlo samples, with M_{top} in the range between 100 and 240 GeV/c^2 , and with the same statistics as the data. Included in these samples is the expected number of background events. The mean of the distribution of the estimated top quark mass for each sample agrees with the generated mass within 2 GeV/c^2 . The average statistical uncertainties derived from the likelihood fits are consistent with the spread of the distributions about 21 GeV/c^2 , and are not strongly dependent on the top quark mass.

Figure 3(a) shows the jet energy distribution of the two highest E_T jets for the eight events in the data overlaid with a template obtained from a combination of $t\bar{t}$ Monte Carlo ($M_{\text{top}} = 160 \text{ GeV}/c^2$) and background in the ratio of 6.7 to 1.3. The distribution of the background alone is also shown. The inset shows the polynomial fit to the $-\ln(\mathcal{L}_m)$ values versus top quark mass. With this method we measure $M_{\text{top}} = 159 \pm 23(\text{stat}) \pm 11(\text{syst}) \text{ GeV}/c^2$.

The second method uses the invariant mass $M_{\ell b}$ of the charged lepton ℓ and the b quark. In the decay of top quarks ($t \rightarrow Wb$), the energy of the b quark in the rest frame of the W boson E_b is a constant ($M_{\text{top}}^2 = M_W^2 + M_b^2 + 2M_W E_b$). With the subsequent semileptonic decay $W \rightarrow \ell\nu$, E_b can be obtained from the invariant mass $M_{\ell b}$ of the charged lepton ℓ and the b quark, and their opening angle $\cos\theta_{\ell b}$. For a sample of $t\bar{t}$ dilepton events, M_{top} is related to $M_{\ell b}$ as $M_{\text{top}}^2 = M_W^2 + \frac{2\langle M_{\ell b}^2 \rangle}{1 - \langle \cos\theta_{\ell b} \rangle}$, where terms that include lepton and b quark masses have been neglected. $\langle M_{\ell b}^2 \rangle$ and $\langle \cos\theta_{\ell b} \rangle$ are the mean values of $M_{\ell b}^2$ and $\cos\theta_{\ell b}$ in the sample. In the standard model tree-level calculation, $\langle \cos\theta_{\ell b} \rangle = M_W^2 / (M_{\text{top}}^2 + 2M_W^2)$, resulting in

$$M_{\text{top}}^2 = \langle M_{\ell b}^2 \rangle + \sqrt{M_W^4 + 4M_W^2\langle M_{\ell b}^2 \rangle + \langle M_{\ell b}^2 \rangle^2}.$$

In each dilepton $t\bar{t}$ candidate, one of the two lepton-jet combinations $(\ell^+ j_1, \ell^- j_2)$, $(\ell^+ j_2, \ell^- j_1)$ corresponds to the correct $(\ell^+ b, \ell^- \bar{b})$ assignment. We select the combination with the smallest sum of invariant masses, result-

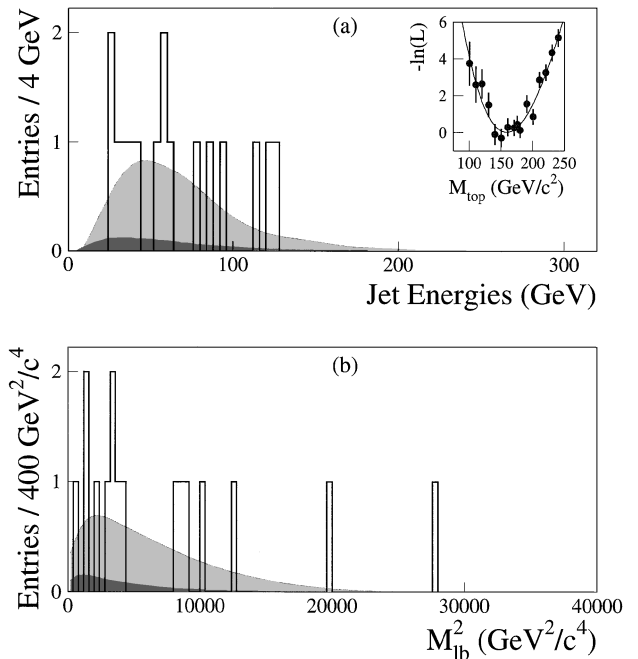


FIG. 3. (a) Jet energy distribution of the two highest E_T jets for the dilepton events (histogram). Superimposed is the same distribution for $t\bar{t}$ Monte Carlo ($M_{\text{top}} = 160 \text{ GeV}/c^2$) plus background (lighter shade) and the background alone (darker shade). The $t\bar{t}$ plus background distribution is normalized to the data. In the inset we show the $-\ln(\mathcal{L}_m)$ fit as a function of M_{top} (the minimum has been offset to be at zero). (b) Distribution of $M_{\ell b-\text{min}}^2$ (histogram). Superimposed is the expectation from $t\bar{t}$ Monte Carlo ($M_{\text{top}} = 160 \text{ GeV}/c^2$) plus background (lighter shade) and the background alone (darker shade).

ing in two values of $M_{\ell b-\text{min}}^2$ per event. The probability of picking up the correct combination is in the range of 55% to 75%, depending on M_{top} . The distribution of $M_{\ell b-\text{min}}^2$ for the eight candidate events is shown in Fig. 3(b) together with the expectation for $M_{\text{top}} = 160 \text{ GeV}/c^2$. The mean value of $M_{\ell b-\text{min}}^2$, $(7.2 \pm 1.9) \times 10^3 \text{ GeV}/c^2$, is used with the linear mapping function, $\langle M_{\ell b}^2 \rangle = C_0 + C_1 \langle M_{\ell b-\text{min}}^2 \rangle$ [with $C_0 = (-2.90 \pm 0.26) \times 10^3$, $C_1 = 1.57 \pm 0.03$], to obtain the value of $\langle M_{\ell b}^2 \rangle$ corresponding to standard model $t\bar{t}$ production and decay. The mapping function is determined from $t\bar{t}$ Monte Carlo events generated with HERWIG and a CDF detector simulation. It accounts for selection biases, incorrect lepton-jet combinations, and jet energy mismeasurements. We obtain $M_{\text{top}} = 163 \pm 20(\text{stat}) \pm 9(\text{syst}) \text{ GeV}/c^2$.

We combine the two mass results by taking into account the correlations in the uncertainties to obtain a single value for the top quark mass, $M_{\text{top}} = 161 \pm 17(\text{stat}) \pm 10(\text{syst}) \text{ GeV}/c^2$. The major contributions to the systematic uncertainty are due to the uncertainty in the jet energy scale and in the shape of the background distributions.

In conclusion, in the dilepton channel we find nine candidate events consistent with originating from $t\bar{t}$ production. The estimated background is 2.4 ± 0.5 events. We

measure the $t\bar{t}$ production cross section to be $8.2^{+4.4}_{-3.4}$ pb for $M_{\text{top}} = 175 \text{ GeV}/c^2$. The measured top quark mass is $M_{\text{top}} = 161 \pm 17(\text{stat}) \pm 10(\text{syst}) \text{ GeV}/c^2$, consistent with the CDF measurement in the lepton plus jets channel of $175.9 \pm 4.8(\text{stat}) \pm 4.9(\text{syst}) \text{ GeV}/c^2$ [11]

We thank the Fermilab staff and the technical staffs of the participating institutions for their contributions. This work was supported by the U.S. Department of Energy and National Science Foundation; the Italian Istituto Nazionale di Fisica Nucleare; the Ministry of Science, Culture, and Education of Japan; the Natural Sciences and Engineering Research Council of Canada; the National Science Council of the Republic of China; and the A. P. Sloan Foundation.

*Visitor.

- [1] F. Abe *et al.*, Phys. Rev. Lett. **74**, 2626 (1995).
- [2] S. Abachi *et al.*, Phys. Rev. Lett. **74**, 2632 (1995).
- [3] F. Abe *et al.*, preceding Letter, Phys. Rev. Lett. **80**, 2773 (1998).
- [4] S. Abachi *et al.*, Phys. Rev. Lett. **79**, 1203 (1997).
- [5] F. Abe *et al.*, this issue, Phys. Rev. Lett. **80**, 2767 (1998).
- [6] S. Abachi *et al.*, Phys. Rev. Lett. **79**, 1197 (1997).

- [7] F. Abe *et al.*, Nucl. Instrum. Methods Phys. Res., Sect. A **271**, 387 (1988).
- [8] In the CDF coordinate system, θ and ϕ are the polar and azimuthal angles, respectively, with respect to the proton beam direction (z axis). The pseudorapidity η is defined as $-\ln \tan(\theta/2)$. The transverse momentum of a particle is $P_T = P \sin \theta$. The analogous quantity using calorimeter energies, defined as $E_T = E \sin \theta$, is called transverse energy. The missing transverse energy \cancel{E}_T is defined as $-\sum E_T^i \hat{n}_i$, where \hat{n}_i is the unit vector in the transverse plane pointing from the interaction point to the energy deposition in calorimeter cell i .
- [9] F. Abe *et al.*, Phys. Rev. D **50**, 2966 (1994); Phys. Rev. Lett. **73**, 225 (1994).
- [10] G. Marchesini and B. R. Webber, Nucl. Phys. B **310**, 461 (1988); G. Marchesini *et al.*, Comput. Phys. Commun. **67**, 465 (1992). We use HERWIG version 5.6.
- [11] M. C. Kruse, Ph.D. thesis, Purdue University, 1996.
- [12] T. Sjöstrand, Comput. Phys. Commun. **82**, 74 (1994). We use PYTHIA version 5.7.
- [13] E. Berger and H. Contopanagos, Phys. Rev. D **54**, 3085 (1996); S. Catani, M. Mangano, P. Nason, and L. Trentadue, Phys. Lett. B **378**, 329 (1996); E. Laenen, J. Smith, and W. L. van Neerven, Phys. Lett. B **321**, 254 (1994).